



Ratchet universality in the directed motion of spheres by unbiased driving forces in viscous fluids

Pedro J. Martínez · Ricardo Chacón

Received: 3 November 2022 / Accepted: 20 April 2023 / Published online: 3 May 2023
© The Author(s) 2023

Abstract Directed motion of a sphere immersed in a viscous fluid and subjected solely to a nonlinear drag force and zero-average biharmonic forces is studied in the absence of any periodic substrate potential. We consider the case of two mutually perpendicular sinusoidal forces of periods T and $T/2$, respectively, which cannot yield any ratchet effect when acting separately, while inducing directed motion by acting simultaneously. Remarkably and unexpectedly, the dependence on the relative amplitude of the two sinusoidal forces of the average terminal velocity is theoretically explained from the theory of ratchet universality, while extensive numerical simulations confirmed its predictions in the adiabatic limit. Additionally, the dependence on the dimensionless driving frequency of the dimensionless average terminal velocity far from the adiabatic limit is

qualitatively explained with the aid of the vibrational mechanics approach.

Keywords Ratchet effect · Viscous fluid · Spheres · Ratchet universality

1 Introduction

Nature's symmetry principles play a subtle and deep role in the sense that many physical phenomena ultimately come to be explained in terms of mechanisms of symmetry breaking. A ubiquitous instance is the so-called ratchet effect [1–3], i.e., the possibility of generating directed transport from a fluctuating environment without any net external force. Indeed, it has been a fundamental research topic in diverse areas of science and technology since the last few decades partly because of its potential applications for manipulating such systems as coupled Josephson junctions [4] and molecular motors [5], as well as for designing micro- and nano-devices suitable for on-chip implementation. Directed ratchet transport (DRT) is now qualitatively understood to be a result of the interplay of nonlinearity, symmetry breaking [6], and non-equilibrium fluctuations including temporal noise [2], spatial disorder [7], and quenched temporal disorder [8]. The symmetry analysis alone, however, is insufficient to predict the strength and direction of the DRT.

P. J. Martínez (✉)
Departamento de Física Aplicada, E.I.N.A, Universidad de Zaragoza, E-50018 Zaragoza, Spain
e-mail: icmat1@unizar.es

R. Chacón
Departamento de Física Aplicada, E.I.I, Universidad de Extremadura, Apartado Postal 382, E-06006 Badajoz, Spain
e-mail: rchacon@unex.es

R. Chacón
Instituto de Computación Científica Avanzada (ICCAEx), Universidad de Extremadura, E-06006 Badajoz, Spain

Recently, some of such fundamental aspects, including current reversals [9] and the quantitative dependence of DRT strength on the system's parameters [10], have begun to be elucidated. In this regard, the theory of *ratchet universality* (RU) [11–13, 13] predicts that there exists a universal force waveform which optimally enhances directed transport by symmetry breaking. The theory of RU is based on a scenario of criticality that emerges when the generalized parity symmetry and the generalized time-reversal symmetry are broken, regardless of the nature of the dynamic equation in which the breaking of such symmetries results in DRT. For noiseless ratchets, the effectiveness of this theory has been demonstrated in quite different physical contexts in which the driving forces are chosen to be biharmonic, such as in the cases of topological solitons [8], Bose–Einstein condensates exposed to a sawtooth-like optical lattice potential [14], matter-wave solitons [10], one-dimensional granular chains [15], and Bose–Einstein condensates under an unbiased periodic driving potential [16]. Thus, the effectiveness of RU in quantum systems has been previously demonstrated, including the cases of directed transport of atoms in a Hamiltonian quantum ratchet (the values of the parameters used, which were chosen to maximize the directed transport, correspond to those of the universal biharmonic waveform, cf. Ref. [14]) and driven Bose–Einstein condensates (the authors show that the ratchet current is maximum for the values of the parameters that correspond to those of the ratchet potential associated with the universal biharmonic waveform, cf. Ref. [16]). There have also been quantitative explanations in coherence with the degree-of-symmetry-breaking mechanism, as predicted by the theory of RU [11, 12], of the interplay between thermal noise and symmetry breaking in the DRT of a Brownian particle moving on a periodic substrate subjected to a homogeneous temporal biharmonic force [17–19] and of a driven Brownian particle subjected to a vibrating periodic potential [20]. Numerical analyses of a driven Brownian particle in the presence of non-Gaussian noise [21], coupled Brownian motors with stochastic interactions in a crowded environment [22], and Stark control of electrons at interfaces [23] have confirmed the RU predictions. Additionally, RU has recently been demonstrated in the bidirectional escape from a symmetric potential well [24], coupled dissipative oscillators without external bias [25] as well as in

directed ratchet transport of cold atoms and fluxons driven by biharmonic fields [26].

2 Theoretical approach and numerical simulation

Here, we investigate the effects of nonlinear dissipative (drag) forces on DRT in the absence of any periodic substrate potential through the recently considered example of spheres immersed in a viscous fluid of viscosity η and density ρ_f , and subjected to time-periodic forces of period T and zero average [27]. In dimensionless variables, the equation of motion reads

$$\omega\tau \frac{d\mathbf{v}(\theta)}{d\theta} = -\frac{1}{24} C_d[|\mathbf{v}(\theta)|]|\mathbf{v}(\theta)|\mathbf{v}(\theta) + f_0\mathbf{f}(\theta), \quad (1)$$

$$\mathbf{f}(\theta) = \zeta \cos(\theta)\mathbf{e}_1 + \alpha(1 - \zeta) \cos(2\theta + \varphi)\mathbf{e}_2, \quad (2)$$

where $\theta \equiv \omega t$, $\omega \equiv 2\pi/T$, $\tau \equiv m/(6\pi r\eta)$ is a characteristic timescale, $\mathbf{v}(\theta) \equiv 2r\rho_f\mathbf{v}(\theta/\omega)/\eta$, $C_d[|\mathbf{v}(\theta)|]$ is the steady drag coefficient, $\mathbf{f}(\theta) \equiv \mathbf{F}(\theta/\omega)/F_0$ with $\mathbf{F}(t)$ being a T -periodic biharmonic force, $f_0 \equiv \rho_f F_0/(3\pi\eta^2)$ is a dimensionless parameter accounting for the strength of the driving force, \mathbf{e}_1 and \mathbf{e}_2 are two mutually perpendicular versors, $\zeta \in [0, 1]$ and $\varphi \in [0, 2\pi]$ accounts for the relative amplitude and initial phase difference of the two harmonic components, respectively, while the value $\alpha = 1$ is the only one considered in Ref. [27]. Note that the dimensionless driving frequency, $\omega\tau = 2\pi(\tau/T)$, accounts for the relative strength of the two timescales involved. An experimental realization of Eq. (1) can be implemented by applying alternating magnetic fields to magnetizable spherical particles in a similar way to the case studied in Ref. [28] (see also Ref. [29]). In the *adiabatic* limit ($\omega\tau \ll 1$), the average terminal velocity, $\bar{\mathbf{v}}_{\text{ad}}$, is given by the integral

$$\bar{\mathbf{v}}_{\text{ad}} = \frac{\delta_0^2 \eta}{16\pi r \rho_f} \int_0^{2\pi} d\theta \left[\sqrt{1 + \frac{4\sqrt{f_0}|\mathbf{f}(\theta)|}{\delta_0}} - 1 \right]^2 \frac{\mathbf{f}(\theta)}{|\mathbf{f}(\theta)|}, \quad (3)$$

with $\delta_0 = 9.06$ [27]. Also, the numerical results discussed in Ref. [27] indicated that, for fixed values

of the other parameters, there exists an optimal value of ζ which maximizes the second component of the dimensionless average terminal velocity, while the maximum velocity decreases as $\omega\tau$ is increased and its location shifts toward lower values of ζ . This present paper aims to provide an explanation of these numerical results for $\alpha = 1$ as well as our own numerical results for any $\alpha > 0$. Specifically, we shall show that the maximum velocity is reached for $\zeta = 2\alpha/(1 + 2\alpha)$ in the adiabatic limit, as predicted by the theory of RU. Indeed, it has been demonstrated for temporal and spatial biharmonic forces that optimal enhancement of directed ratchet transport is achieved when maximally effective (i.e., *critical*) symmetry breaking occurs, which implies the existence of a particular universal waveform [11–13]. Specifically, the optimal value of the relative amplitude ζ comes from the condition that the amplitude of the odd harmonic component must be twice that of the even harmonic component in Eq. (2), i.e.,

$$\zeta_{\text{opt}} = \zeta_{\text{opt}}(\alpha) \equiv 2\alpha/(1 + 2\alpha). \tag{4}$$

Importantly, this finding is in sharp contrast to the prediction coming from the general formalism mentioned in Ref. [27], namely, that the dependence of the average terminal velocity should scale as

$$\bar{V}_2(\zeta) \approx C\zeta^2\alpha(1 - \zeta),$$

where C is independent of ζ . This equation indicates that $\bar{V}_2(\zeta)$ presents a single maximum at $\zeta_{\text{max}} = 2/3$, *irrespective* of the particular value of the prefactor α . Note that the coincidence of $\zeta_{\text{max}} = 2/3$ with $\zeta_{\text{opt}}(\alpha = 1)$ is purely accidental (see Appendix A). In contrast, both the theoretical estimate given by Eq. (3) and numerical simulations of Eq. (1) confirm the RU prediction [Eq. (4)] over a wide range of α values (cf. Figures 1 top and bottom, respectively).

Figure 2 is the same as Fig. 1 but for a much lower dimensionless driving strength ($f_0 = 1$). One sees that the theoretical estimate given by Eq. (3) and numerical simulations of Eq. (1) again confirm the RU prediction [Eq. (4)] over the same range of α values (cf. Figures 2 top and bottom, respectively). Note that the average terminal velocity increases as the prefactor α is increased, while keeping the remaining parameters constant (cf. Figures 1 and 2), because the condition $|\mathbf{f}(\theta)| \leq 1$ is no longer satisfied for $\alpha > 1$ and the

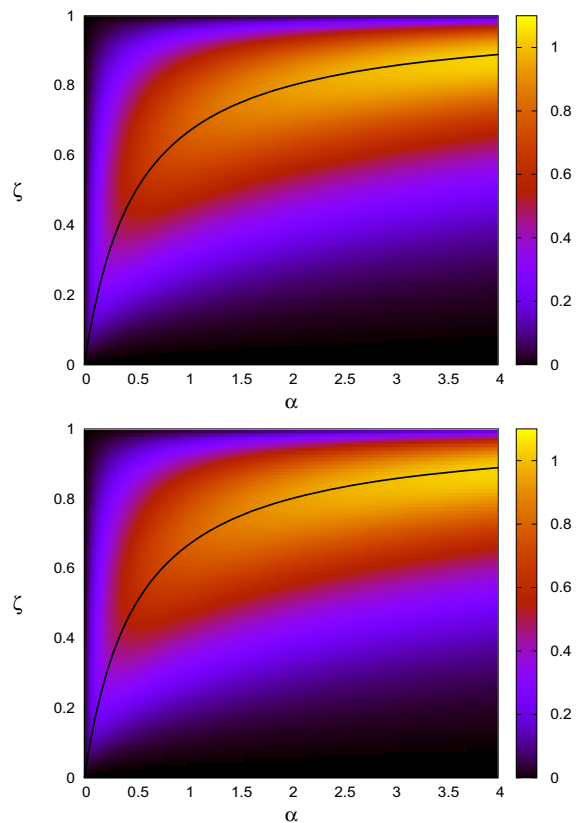


Fig. 1 Dimensionless average terminal velocity versus relative amplitude ζ and prefactor α [cf. Equation (2)] for $f_0 = 100$, $\omega\tau = 0.1$, and $\varphi = \pi$. Top: Theoretical prediction from Eq. (3). Bottom: Numerical results from Eqs. (1) and (2). Also plotted is the theoretical prediction for the maximum velocity [cf. Equation (4); solid curve]

particular value of F_0 considered in Ref. [27] for $\alpha = 1$.

For the sake of making a legitimate comparison, Fig. 3 shows the corresponding results after the substitution $\mathbf{f}(\theta) \rightarrow \mathbf{f}(\theta)/M$ with

$$M = |\mathbf{f}(\theta)|_{\text{max}} \equiv \sqrt{\zeta^2 + \alpha^2(1 - \zeta)^2} \tag{5}$$

such that $|\mathbf{f}(\theta)|/M \leq 1$. Clearly, the RU prediction presents excellent agreement with the results from numerical simulations for quite disparate values of f_0 (cf. Figures 3 middle and bottom) as well as with the theoretical estimate [Eq. (3); Fig. 3 top]. Note, however, that such an excellent agreement between RU prediction and numerical results would not be expected *a priori* in the present case of two mutually

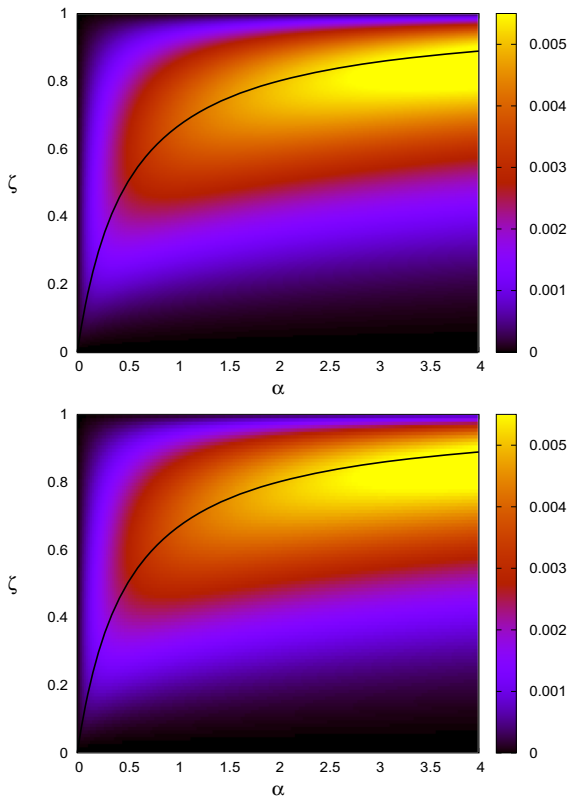


Fig. 2 The same as Fig. 1, but now $f_0 = 1$

perpendicular sinusoidal forces, one with twice the period of the other.

The effectiveness of the RU prediction [Eq. (4)] can be understood as follows. In the adiabatic limit ($\omega\tau \ll 1$), after substituting

$$v_{ad}(\theta) = \frac{\delta_0^2}{4} \left[\sqrt{1 + \frac{4\sqrt{f_0}|\mathbf{f}(\theta)|}{\delta_0}} - 1 \right]^2 \frac{\mathbf{f}(\theta)}{|\mathbf{f}(\theta)|} \tag{6}$$

(cf. Equation (11) of Ref. [27]) into the expression $C_d[|v_{ad}(\theta)|]|v_{ad}(\theta)|v_{ad}(\theta)$ with the assumption $v_{ad}(\theta) \propto \mathbf{f}(\theta)$, and Taylor- and Fourier-expanding the nonlinear part of this friction force, for instance for $\varphi = \varphi_{opt} \equiv \pi$ (see Appendix B), Eq. (1) can be written as

$$\omega\tau \frac{dv_1}{d\theta} = -v_1 - A \sum_{n=1}^{\infty} b_{2n-1} \cos[(2n-1)\theta] + f_0\zeta \cos \theta, \tag{7}$$

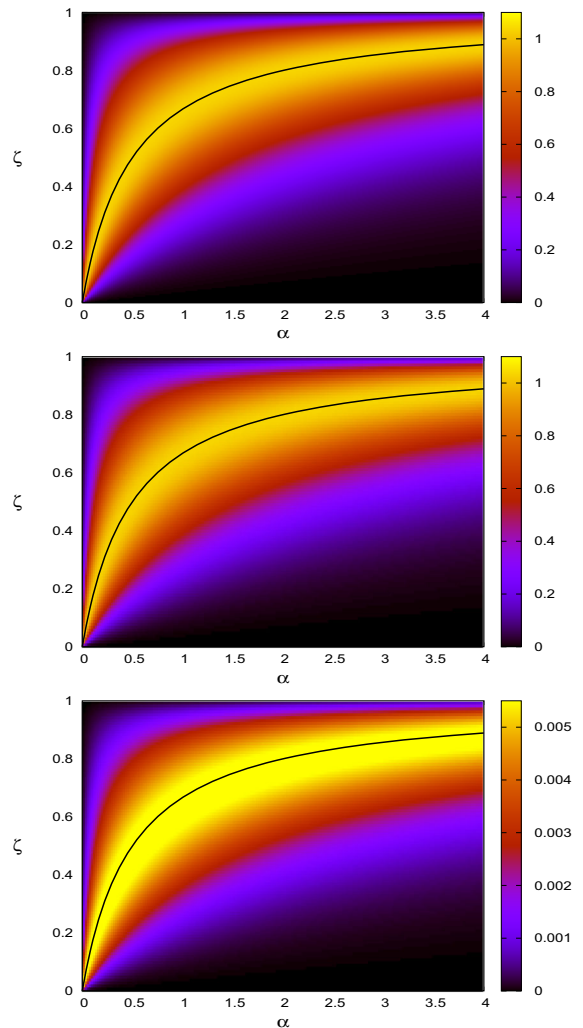


Fig. 3 Dimensionless average terminal velocity versus relative amplitude ζ and prefactor α [cf. Equation (2)] for $\omega\tau = 0.1$ and $\varphi = \pi$. Top: Theoretical prediction from Eq. (3) for $f_0 = 100$. Middle: Numerical results from Eqs. (1) and (2) after the substitution $\mathbf{f}(\theta) \rightarrow \mathbf{f}(\theta)/M$ [cf. Equation (5)] for $f_0 = 100$. Bottom: Numerical results from Eqs. (1) and (2) after the substitution $\mathbf{f}(\theta) \rightarrow \mathbf{f}(\theta)/M$ [cf. Equation (5)] for $f_0 = 1$. Also plotted is the theoretical prediction for the maximum velocity [cf. Equation (4); solid curve]

$$\omega\tau \frac{dv_2}{d\theta} = -v_2 - A \sum_{n=0}^{\infty} a_{2n} \cos(2n\theta) - f_0\alpha(1 - \zeta) \cos(2\theta), \tag{8}$$

where $A = A(\delta_0, f_0) \propto 2f_0^{1/4}\delta_0^{-1/2}$, while the Fourier coefficients $a_{2n} \equiv a_{2n}(\zeta, \alpha)$, $b_{2n-1} \equiv b_{2n-1}(\zeta, \alpha)$ can be calculated explicitly by using MATHEMATICA, but their size and algebraic complexity prevent us

from showing them easily. One sees that the net periodic force in Eq. (7) only presents odd harmonics and hence satisfies the shift symmetry, which means that, as expected from the symmetry analysis in Ref. [27], such a periodic force by itself cannot yield directed ratchet motion in the \mathbf{e}_1 direction. Also, the net force in Eq. (8) only presents even harmonics and a constant force term

$$-Aa_0 \approx \frac{2f_0^{1/4}}{\sqrt{\delta_0}} \sum_{k=0}^{\infty} \sum_{n=0}^k \frac{\binom{k}{n} \zeta^{2k-2n} \alpha^{2n+1} (1-\zeta)^{2n+1} c(k,n)}{\Gamma(\frac{1}{8}-k+1)k! [\zeta^2 + \alpha^2(1-\zeta)^2]^k}, \tag{9}$$

with

$$c(k,n) \equiv \Delta_{k,n} \left[\sqrt{\pi_2} \tilde{F}_1 \left(\frac{1}{2}, \frac{k+n+3}{2}; n+\frac{3}{2}; -1 \right) + (-1)^n {}_2\tilde{F}_1 \left(\frac{k-n+2}{2}, \frac{k+n+3}{2}; \frac{k+n+4}{2}; -1 \right) \Gamma \left(\frac{k-n+2}{2} \right) \right] \tag{10}$$

where $\Delta_{k,n} \equiv (-1)^{-n} [(-1)^n - (-1)^k] \Gamma(n+1)$ while $\Gamma(\cdot)$ and ${}_2\tilde{F}_1(\cdot, \cdot; \cdot; \cdot)$ are the gamma and the regularized hypergeometric functions, respectively. Since the waveform of any pair of even harmonics $a_{2n} \cos(2n\theta) + a_{2n+2} \cos[(2n+2)\theta]$ in Eq. (8) does not fit, for any value of ζ, α , that of one of the four equivalent expressions of the biharmonic universal excitation [11]

$$f_0 \left[\sin \theta \pm \frac{1}{2} \sin(2\theta) \right], \tag{11}$$

$$f_0 \left[\cos \theta \pm \frac{1}{2} \sin(2\theta) \right],$$

this means that the emergence of directed ratchet motion in the \mathbf{e}_2 direction is exclusively due to the constant force $-Aa_0$ which is given approximately by Eq. (9) for the parameters used in Fig. 3 of Ref. [27]. Indeed, the RU prediction [Eq. (4)] presents good agreement with the theoretical estimate of the constant force arising from the Fourier analysis of the net force [cf. Equation (9); see Fig. 4] because the universal

biharmonic waveform is effectively present to produce the term of constant force *once* $\mathbf{f}(\theta)$ has been suitably normalized as in the criticality scenario leading to ratchet universality [12]. Mathematically, Eqs. (7) and (8) are two nonautonomous (decoupled) linear equations, and hence the expected average terminal velocities are $\bar{v}_1 = 0, \bar{v}_2 = -Aa_0$, thus explaining the aforementioned agreement.

Next, the aforementioned dependence of the location of the maximum velocity on $\omega\tau$ can be understood as follows. First, we rewrite Eq. (1) as

$$\frac{d\mathbf{v}(\Omega t_\tau)}{dt_\tau} = -\frac{1}{24} C_d [|\mathbf{v}(\Omega t_\tau)|] |\mathbf{v}(\Omega t_\tau)| \mathbf{v}(\Omega t_\tau) + f_0 [\zeta \cos(\Omega t_\tau) \mathbf{e}_1 + \alpha(1-\zeta) \cos(2\Omega t_\tau + \varphi) \mathbf{e}_2], \tag{12}$$

where $\Omega \equiv \omega\tau, t_\tau \equiv t/\tau$. For sufficiently large Ω , i.e., when $2\pi < T/\tau < 4\pi$, the v_2 dynamics of Eq. (12) can be analyzed using the vibrational mechanics approach [30] by assuming that the Ω -force is “slow” ($\Omega < 1$) while the 2Ω -force is “fast” ($2\Omega > 1$). Thus, one separates $v_2(t_\tau) = V_2(t_\tau) + \psi(t_\tau)$, where $V_2(t_\tau)$ represents the slow dynamics while $\psi(t_\tau)$ is the fast oscillating term (see Appendix B): $\psi(t_\tau) = \psi_0 \cos(2\Omega t_\tau + \Phi)$ with

$$\psi_0 \equiv f_0 \alpha (1-\zeta) / \sqrt{1+4\Omega^2}, \tag{13}$$

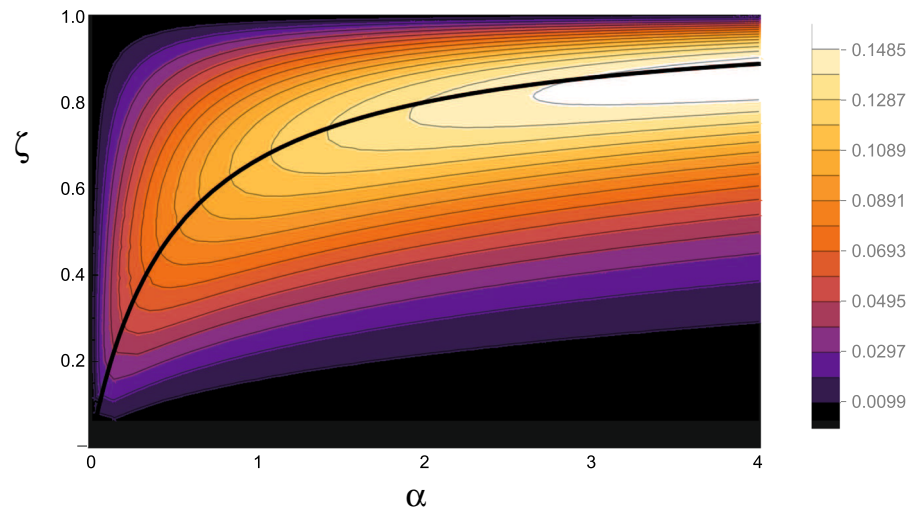
$$\Phi \equiv \arctan \left[\frac{\text{tg } \varphi - 2\Omega}{1+2\Omega \text{tg } \varphi} \right].$$

On averaging out $\psi(t_\tau)$ over time $2\Omega t_\tau$, the slow reduced dynamics of v_2 becomes

$$\frac{dV_2}{dt_\tau} + V_2 \left(1 + \frac{4\pi}{\delta_0} \sqrt{|V_2|} \right) = 0. \tag{14}$$

Thus, the asymptotic v_2 dynamics when $\Omega \equiv \omega\tau \gg 1/2$ could well be described by Eq. (14), which indicates that the (terminal) velocity $V_2 \sim e^{-t/\tau}$ as $t \rightarrow \infty$. This scenario is coherent with the gradual decrease of the maximum second component of the dimensionless average terminal velocity (cf. Figure 3 in Ref. [27]) as $\omega\tau$ is increased from the adiabatic limit, i.e., as the relevant symmetries are *gradually* restored. This phenomenon of competing timescales leads to the 2Ω -force losing ratchet effectiveness, but without deactivating the degree-of-symmetry-breaking mechanism [11, 12]. Clearly, this loss of effectiveness can only be compensated by increasing its

Fig. 4 Estimation of the constant term $-Aa_0$ after retaining only the first six terms versus relative amplitude ζ and prefactor α [cf. Equation (9)] for $f_0 = 100$. Also plotted is the theoretical prediction for the maximum velocity [cf. Equation (4); solid curve]



amplitude $\alpha(1 - \zeta)$ to generate maximum velocity, thereby explaining the shift of the location of the maximum velocity to lower values of ζ as $\omega\tau$ is increased from the adiabatic limit (cf. Figure 3 in Ref. [27]). Importantly, this does not mean that the predictions of the theory of RU are not universal but there is another phenomenon that affects directed transport and interacts with the breaking of the relevant symmetries. A similar situation occurs when thermal noise is present in a directed transport scenario (see Refs. [17–19]).

3 Conclusions

In summary, we have investigated directed ratchet motion of a sphere immersed in a viscous fluid and subjected solely to a nonlinear drag force and zero-average biharmonic forces in the absence of any periodic substrate potential. The dependence on the relative amplitude of two mutually perpendicular sinusoidal forces of the average terminal velocity was theoretically explained from the theory of ratchet universality, while extensive numerical simulations fully confirmed its predictions in the adiabatic limit. Also, the dependence on the dimensionless driving frequency of the dimensionless average terminal velocity far from the adiabatic limit was qualitatively explained with the aid of the vibrational mechanics approach, while a quantitative explanation for such

behavior is still lacking. The theoretical findings of this article could stimulate further experimental work on directed ratchet transport of particles in non-Newtonian fluids. Finally, following the present Fourier series expansion approach, we expect that the theory of RU will explain other different implementations of the ratchet effect, such as gating ratchets [31] and skyrmion ratchets [32]. Our current work is aimed at exploring these cases.

Funding Open Access funding provided thanks to the CRUE-CSIC agreement with Springer Nature. P.J.M. acknowledges Grant No. PID2020-113582GB-100 funded by Spanish MCIN/AEI/10.13039/501100011033 and by “ERFD A way of making Europe” and also to Gobierno de Aragón (DGA, Spain) through Project No. E36_23R. R.C. acknowledges financial support from the Junta de Extremadura (JEx, Spain) through Project No. GR21012 cofinanced by FEDER funds.

Data availability statement The datasets generated during and/or analyzed during the current study are available from the corresponding author on reasonable request.

Declarations

Conflict of interest The authors declare that they have no conflict of interest.

Open Access This article is licensed under a Creative Commons Attribution 4.0 International License, which permits use, sharing, adaptation, distribution and reproduction in any medium or format, as long as you give appropriate credit to the original author(s) and the source, provide a link to the Creative Commons licence, and indicate if changes were made. The

images or other third party material in this article are included in the article’s Creative Commons licence, unless indicated otherwise in a credit line to the material. If material is not included in the article’s Creative Commons licence and your intended use is not permitted by statutory regulation or exceeds the permitted use, you will need to obtain permission directly from the copyright holder. To view a copy of this licence, visit <http://creativecommons.org/licenses/by/4.0/>.

Appendix A

Let us consider the following reparameterization of the biharmonic force [cf. Equations (1) and (2)]:

$$f_0[\zeta \cos(\theta)\mathbf{e}_1 + \alpha(1 - \zeta) \cos(2\theta + \varphi)\mathbf{e}_2] = f'_0[\zeta' \cos(\theta)\mathbf{e}_1 + (1 - \zeta') \cos(2\theta + \varphi)\mathbf{e}_2], \tag{A1}$$

i.e.,

$$f'_0 \equiv f_0[\zeta + \alpha(1 - \zeta)], \tag{A2}$$

$$\zeta' \equiv [1 + \alpha(1 - \zeta)/\zeta]^{-1}. \tag{A3}$$

The general formalism mentioned in Ref. [27] predicts that the dependence of the average terminal velocity should scale as

$$\bar{V}_2(\zeta) \approx f_0^3 \alpha \zeta^2 (1 - \zeta) \tag{A4}$$

and

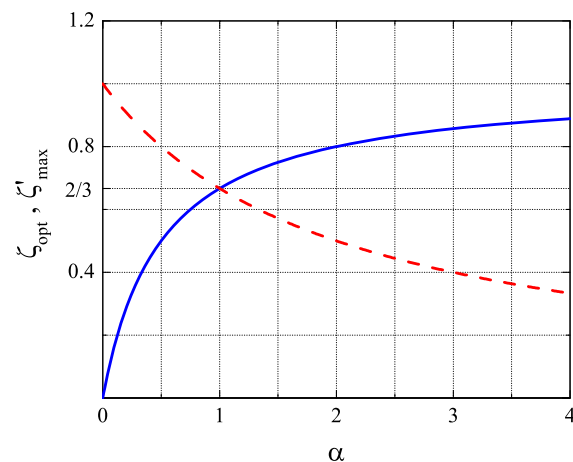


Fig. 5 Functions $\zeta_{\text{opt}}(\alpha)$ [Eq. (4), solid line] and $\zeta'_{\text{max}}(\alpha)$ [Eq. (A6), dashed line] vs prefactor α

$$\bar{V}_2(\zeta') \approx f_0^3 \frac{\alpha^3 (1 - \zeta') \zeta'^2}{[1 + (\alpha - 1)\zeta']^3} \tag{A5}$$

as a function of ζ and ζ' , respectively. Clearly, $\bar{V}_2(\zeta')$ presents a single maximum at

$$\zeta' = \zeta'_{\text{max}}(\alpha) \equiv 2/(2 + \alpha), \tag{A6}$$

which only matches the correct dependence $2\alpha/(1 + 2\alpha)$ [cf. Equation (4), see Fig. 3] when $\alpha = 1$ (see Fig. 5).

Appendix B

For the parameters considered in Ref. [27] ($\delta_0 = 9.06, f_0 = 100$), one readily obtains

$$|v_{\text{ad}}(\theta)| \approx \delta_0 \sqrt{f_0} |\mathbf{f}(\theta)|^{1/2} \tag{B1}$$

from Eq. (6), and hence Eq. (1) can be approximated in the adiabatic limit as

$$\omega\tau \frac{dv_{\text{ad}}(\theta)}{d\theta} = -v_{\text{ad}}(\theta) - \frac{2f_0^{1/4}}{\sqrt{\delta_0}} |\mathbf{f}(\theta)|^{1/4} v_{\text{ad}}(\theta) + f_0 \mathbf{f}(\theta), \tag{B2}$$

where $\mathbf{f}(\theta)$ is given by Eq. (2). Thus, after assuming

$$v_{\text{ad}}(\theta) = \kappa \mathbf{f}(\theta) / M^{1/4} \tag{B3}$$

[cf. Equation (5)] in the nonlinear friction term $2f_0^{1/4} \delta_0^{-1/2} |\mathbf{f}(\theta)|^{1/4} v_{\text{ad}}(\theta)$ with κ being a fitting constant (see Fig. 6) and, for instance, $\varphi = \varphi_{\text{opt}} \equiv \pi$, Eq. (B2) can be recast into the form

$$\omega\tau \frac{dv_1}{d\theta} = -v_1 - \frac{2\kappa f_0^{1/4}}{\sqrt{\delta_0}} F_1(\theta, \zeta, \alpha) + f_0 \zeta \cos \theta, \tag{B4}$$

$$\omega\tau \frac{dv_2}{d\theta} = -v_2 - \frac{2\kappa f_0^{1/4}}{\sqrt{\delta_0}} F_2(\theta, \zeta, \alpha) - f_0 \alpha (1 - \zeta) \cos(2\theta), \tag{B5}$$

with

$$F_1(\theta, \zeta, \alpha) \equiv \frac{\zeta \cos \theta}{2^{1/8}} \left[1 + \frac{\zeta^2 \cos(2\theta) + \alpha^2 (1 - \zeta)^2 \cos(4\theta)}{\zeta^2 + \alpha^2 (1 - \zeta)^2} \right]^{1/8}, \tag{B6}$$

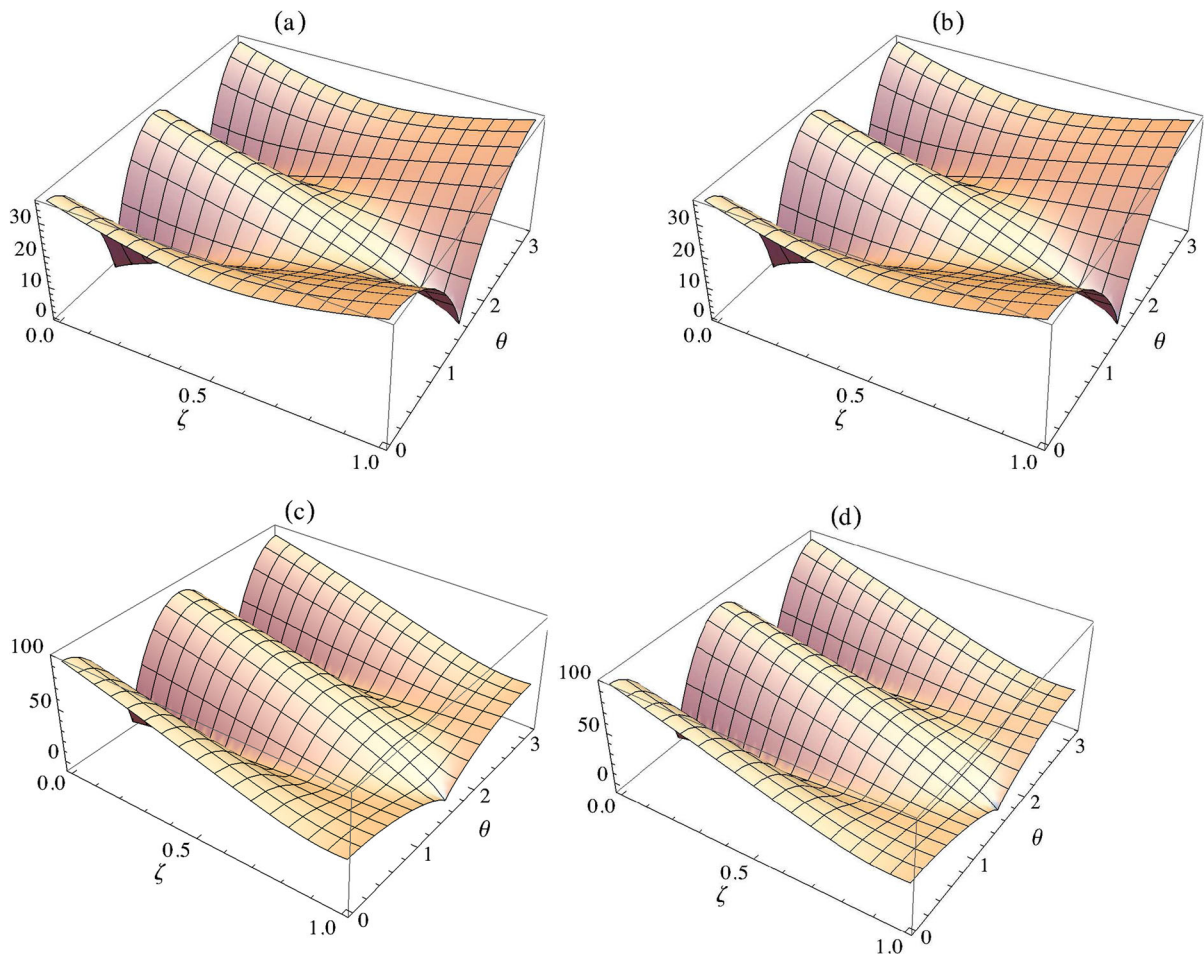


Fig. 6 Dimensionless terminal velocity in the adiabatic limit v_{ad} versus relative amplitude ζ and phase θ from **a, c** Eq. (6) and **b, d** Eq. (B3) for $f_0 = 100$, $\delta = 9.06$, $\varphi = \pi$, and two values of

the prefactor α : **a, b** $\alpha = 1$ and **c, d** $\alpha = 4$. Fitting constant [cf. Equation (B3)]: **b** $\kappa = 36.6$, **d** $\kappa = 33.6$

$$F_2(\theta, \zeta, \alpha) \equiv -\frac{\alpha(1-\zeta)\cos(2\theta)}{2^{1/8}} \left[1 + \frac{\zeta^2 \cos(2\theta) + \alpha^2(1-\zeta)^2 \cos(4\theta)}{\zeta^2 + \alpha^2(1-\zeta)^2} \right]^{1/8} \tag{B7}$$

Finally, after Taylor- and Fourier-expanding $F_{1,2}(\theta, \zeta, \alpha)$ in Eqs. (B4) and (B5) with the aid of MATHEMATICA, one straightforwardly obtains Eqs. (7) and (8), respectively. Since the fitting constant κ [cf. Equation (B3)] decreases very slowly with α ($(\kappa(\alpha = 1) - \kappa(\alpha = 4))/\kappa(\alpha = 1) \simeq 0.082$ for the cases shown in Fig. 6), the right-hand side of Eq. (9) effectively account for the dependence on α of the constant force term, which is indeed confirmed by the estimate shown in Fig. 4.

Next, we discuss the application of the vibrational mechanics approach [30] to the v_2 dynamics of

Eq. (12). For the aforementioned parameters considered in Ref. [27], the respective equation of motion can be approximated as

$$\frac{dv_2}{dt_\tau} + \left(1 + \frac{2}{\delta_0} \sqrt{|v|} \right) v_2 = -f_0 \alpha (1 - \zeta) \cos(2\Omega t_\tau). \tag{B8}$$

After assuming $2\pi < T/\tau < 4\pi$, i.e. that the Ω -force is “slow” while the 2Ω -force is “fast”, one separates

$$v_2(t_\tau) = V_2(t_\tau) + \psi(t_\tau), \tag{B9}$$

where $V_2(t_\tau)$ represents the slow dynamics while $\psi(t_\tau)$ is the fast oscillating term. Note that $V_2(t_\tau)$ is the main component, while $\psi(t_\tau)$ satisfies the condition

$$\langle \psi \rangle \equiv \int_0^{2\pi} \psi(t_\tau) d(2\Omega t_\tau) = 0 \quad (\text{B10})$$

and it is considered small as compared to $V_2(t_\tau)$. Thus, after substituting Eq. (B9) in Eq. (B8), the equations of fast and slow motions read

$$\frac{d\psi}{dt_\tau} + \psi = -f_0\alpha(1 - \zeta) \cos(2\Omega t_\tau) + O(2/\delta_0), \quad (\text{B11})$$

$$\frac{dV_2}{dt_\tau} + V_2 = -\frac{2}{\delta_0} \left\langle |v_1^2 + (V_2 + \psi)^2|^{1/4} (V_2 + \psi) \right\rangle, \quad (\text{B12})$$

respectively. Since $2/\delta_0$ is sufficiently small, the 2π -periodic solution of Eq. (B11) becomes

$$\psi(t_\tau) = \psi_0 \cos(2\Omega t_\tau + \Phi) \quad (\text{B13})$$

with ψ_0 and Φ given by Eq. (13). After substituting Eq. (B13) in Eq. (B12), on averaging out $\psi(t_\tau)$ over time $2\Omega t_\tau$, and taking into account that $v_1, \langle \psi^2 \rangle \ll V_2$, one obtains Eq. (14).

References

- Feynman, R.P., Leighton, R.B., Sands, M.: The Feynman Lectures on Physics. Addison Wesley, Boston (1964)
- Reimann, P.: Brownian motors: noisy transport far from equilibrium. *Phys. Rep.* **361**, 57–265 (2002)
- Tarlie, M.B., Astumian, R.D.: Optimal modulation of a Brownian ratchet and enhanced sensitivity to a weak external force. *Proc. Natl. Acad. Sci. U.S.A.* **95**, 2039 (1998)
- Li, J.-H.: Superconducting junctions perturbed by environmental fluctuation. *Phys. Rev. E* **67**, 061110 (2003)
- Jülicher, F., Ajdari, A., Prost, J.: Modeling molecular motors. *Rev. Mod. Phys.* **69**, 1269–1281 (1997)
- Flach, S., Yevtushenko, O., Zolotaryuk, Y.: Directed current due to broken time-space symmetry. *Phys. Rev. Lett.* **84**, 2358–2361 (2000)
- Kolton, A.B.: Transverse rectification of disorder-induced fluctuations in a driven system. *Phys. Rev. B* **75**, 020201(R) (2007)
- Martínez, P.J., Chacón, R.: Disorder induced control of discrete soliton ratchets. *Phys. Rev. Lett.* **100**, 144101 (2008)
- Arzola, A.V., Volke-Sepúlveda, K., Mateos, J.L.: Experimental control of transport and current reversals in a deterministic optical rocking ratchet. *Phys. Rev. Lett.* **106**, 168104 (2011)
- Rietmann, M., Carretero-González, R., Chacón, R.: Controlling directed transport of matter-wave solitons using the ratchet effect. *Phys. Rev. A* **83**, 053617 (2011)
- Chacón, R.: Optimal control of ratchets without spatial asymmetry. *J. Phys. A: Math. Theor.* **40**, F413–F419 (2007)
- Chacón, R.: Criticality-induced universality in ratchets, *J. Phys. A: Math. Theor.* **43**, 322001 (2010); Chacón, R.: Corrigendum: Criticality-induced universality in ratchets (2010 *J. Phys. A: Math. Theor.* **43** 322001), *J. Phys. A: Math. Theor.* **54**, 209501 (2021)
- Chacón, R., Martínez, P.J.: Exact universal excitation waveform for optimal enhancement of directed ratchet transport. *Int. J. Bifurc. Chaos* **31**(7), 2150109 (2021)
- Salger, T., Kling, S., Hecking, T., Geckeler, C., Morales-Molina, L., Weitz, M.: Directed transport of atoms in a Hamiltonian quantum ratchet. *Science* **326**, 1241–1243 (2009)
- Berardi, V., Lydon, J., Kevrekidis, P.G., Daraio, C., Carretero-González, R.: Directed ratchet transport in granular chains. *Phys. Rev. E* **88**, 052202 (2013)
- Creffield, C.E., Sols, F.: Coherent ratchets in driven Bose-Einstein condensates. *Phys. Rev. Lett.* **103**, 200601 (2009)
- Martínez, P.J., Chacón, R.: Ratchet universality in the presence of thermal noise. *Phys. Rev. E* **87**, 062114 (2013)
- Martínez, P.J., Chacón, R.: Erratum: Ratchet universality in the presence of thermal noise. *Phys. Rev. E* **88**, 019902 (2013)
- Martínez, P.J., Chacón, R.: Reply to “Comment on Ratchet universality in the presence of thermal noise”. *Phys. Rev. E* **88**, 066102 (2013)
- Chacón, R., Martínez, P.J.: Controlling directed ratchet transport of driven overdamped Brownian particles subjected to a vibrating periodic potential: Ratchet universality versus harmonic-mixing perturbation theory. *Nonlinear Dyn.* **104**, 2411 (2021)
- Xu, J., Luo, X.: Ratchet effects of a Brownian particle with non-Gaussian noise driven by a biharmonic force. *Mod. Phys. Lett. B* **33**, 1950230 (2019)
- Lin, L., Yu, L., Lv, W., Wang, H.: Ratchet motion and current reversal of Brownian motors coupled by birth-death interactions in the crowded environment. *Chin. J. Phys.* **68**, 808–819 (2020)
- Garzón-Ramírez, A.J., Franco, I.: Symmetry breaking in the Stark control of electrons at interfaces (SCELI). *J. Chem. Phys.* **153**, 044704 (2020)
- Chacón, R., Martínez, P.J., Marcos, J.M., Aranda, F.J., Martínez, J.A.: Ratchet universality in the bidirectional escape from a symmetric potential well. *Phys. Rev. E* **103**, 022203 (2021)
- Martínez, P.J., Chacón, R.: Ratchet universality in coupled oscillators without external bias. *Phys. Rev. E* **104**, 024224 (2021)
- Chacón, R., Martínez, P.J.: Directed ratchet transport of cold atoms and fluxons driven by biharmonic fields: a unified view. *Phys. Rev. E* **104**, 014120 (2021)
- Casado-Pascual, J.: Directed motion of spheres induced by unbiased driving forces in viscous fluids beyond the Stokes’ law regime. *Phys. Rev. E* **97**, 032219 (2018)
- Camacho, G., Rodríguez-Barroso, A., Martínez-Cano, O., Morillas, J.R., Tierno, P., de Vicente, J.: Experimental

- realization of a colloidal ratchet effect in a non-Newtonian fluid. *Phys. Rev. Appl.* **19**, L021001 (2023)
29. Chhabra, R.P.: *Bubbles, Drops, and Particles in Non-Newtonian Fluids*, 2nd edn. CRC Press, Boca Raton (2007)
 30. Blekhman, I.I.: *Vibrational Mechanics*. World Scientific, Singapore (2000)
 31. Gommers, R., Lebedev, V., Brown, M., Renzoni, F.: Gating Ratchets for cold atoms. *Phys. Rev. Lett.* **100**, 040603 (2008)
 32. Chen, W., Liu, L., Ji, Y., Zheng, Y.: Skyrmion ratchet effect driven by a biharmonic force. *Phys. Rev. B* **99**, 064431 (2019)

Publisher's Note Springer Nature remains neutral with regard to jurisdictional claims in published maps and institutional affiliations.